

A new descriptor for retrieving 3D objects applied in Congestive Heart Failure diagnosis

Helton H. BÍscaro, Hellyan Oliveira, Leila C. C. Bergamasco, Fátima L. S. Nunes
Laboratory of Computer Applications for HealthCare
School of Arts, Sciences and Humanities, Polytechnic School
University of São Paulo
São Paulo, Brazil
Emails: heltonhb@usp.br, leila.cristina@usp.br, fatima.nunes@usp.br

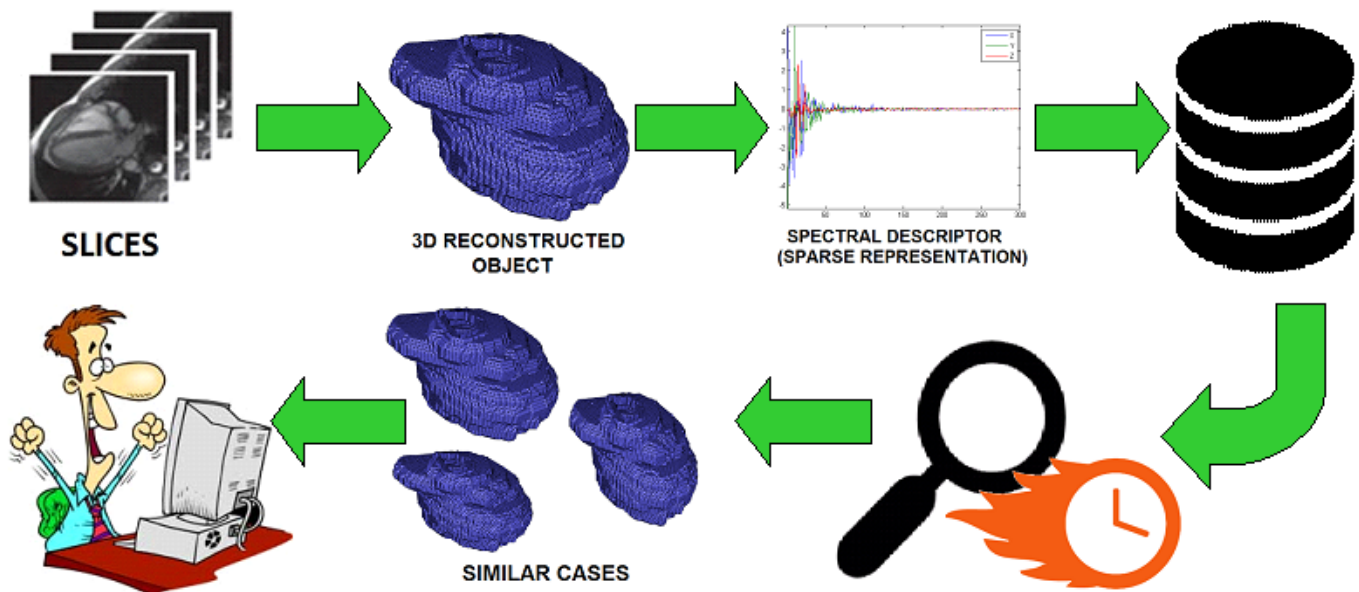


Fig. 1. The Spectral Descriptor: the process of extracting data from the 3D object is shown in the first line; the second line illustrates how the retrieval can be faster with this descriptor.

Abstract—Content-Based Image Retrieval (CBIR) aims to retrieve similar graphical objects from large databases based on their contents. CBIR requires definition of descriptors, algorithms that condense information from the object in order to represent it usually as a real number or a vector in \mathbb{R}^n . This article presents the Spectral Descriptor, a new descriptor designed for retrieving three-dimensional geometric objects applied to aid the diagnosis of Congestive Heart Failure (CHF). Our descriptor is based on techniques of compressive sensing and rewrites the coordinates of 3D objects vertices on a basis on which they have a sparse representation. Tests with surfaces reconstructed from heart MRI images, specifically from left ventricle, show that the descriptor has presented a good performance, reaching an average precision of approximately 85% for CHF and 71% for non-CHF cases, maintaining high levels of precision. Results also showed that the Spectral Descriptor can decrease the high dimensionality of features vectors in CBIR systems.

Keywords—Content-Based Image Retrieval (CBIR); Spectral Descriptor; Three-dimensional Objects; Congestive Heart Failure

I. INTRODUCTION

Medical images and objects, regarding to two-dimensional (2D) and three-dimensional (3D) domains respectively, are increasingly common in health area aiming at aiding the diagnosis. However, these objects generate a huge volume of data to be constantly stored and retrieved, becoming unfeasible finding similar cases by manually querying the set of objects.

Content-based image retrieval (CBIR) has been investigated to minimize this problem. Its goal is finding in an image database the most similar objects to an object provided as a query object. To reach this goal, CBIR extracts characteristics from the object by using algorithms named descriptors, forms

a vector with the extracted characteristics and applies methods to measure the similarity among objects. Considering the health context, CBIR has been well explored in 2D domain, but the complexity of 3D domain objects has limited its applications.

Three-dimensional cardiac objects are commonly used in the clinical day-to-day to aid the diagnosis of heart diseases. Usually they are reconstructed from slices obtained by Magnetic Resonance Imaging (MRI) or Computed Tomography (CT). As other health areas, the volume of data stored is huge and it is not trivial to find specific cases in the images database. At the same time, retrieving similar cases can be an efficient strategy to aid to compose a diagnosis.

Some cardiac diseases present change in the shape of the heart, which can be better observed in 3D objects than in 2D slices sequence. An example is the Congestive Heart Failure (CHF), which present changes mainly on the left ventricle. A CBIR system to retrieve cases similar to one provided as a query object can be an important tool to aid the diagnosis of this anomaly.

This work presents a new descriptor named Spectral Descriptor aiming at extracting features from 3D objects to represent them and, thus, contribute to efficient retrieval. We applied this descriptor to compare shapes of different left ventricles to aid the diagnosis of CHF. However, it can be applied in any problem with the same nature, i.e., problems where someone desires retrieve similar 3D objects from a database considering similarity among their shapes. The descriptor uses a singular value decomposition (SVD) in a Laplacian matrix computed from the 3D geometric objects in order to evaluate its Spectral Coordinates.

This descriptor relay on two basic ideas: *sparsity* as well as *incoherence*. **Sparsity** expresses the idea that the number of degrees of freedom of a known signal is significantly smaller than its length. Many natural signals such as images, sounds and, specially, geometrical meshes are sparse or they have a sparse representation in a proper basis. **Incoherence** extends the duality between time and frequency. The basic idea is that signals that have a sparse representation in a specific basis must be spread out of this domain.

According to the work of Schulz, Velho and Silva [1], some authors describe this duality as a Uniform Uncertainty Principle (UUP) which guarantees that a signal cannot be simultaneously dense in both two domains.

Initial results show that its performance is high, even for high values of recall. The novelty presented in this paper, in addition to the descriptor itself, is its use in the CBIR's context, particularly to be used in a computer-aided diagnosis system.

II. BACKGROUND

In a previous work, Emannuel J. Candès [2] suggests the possibility of new data acquisition protocols that translate analogical information into digital information with less sensors than it was previously considered necessary. In the same work, the author provides the key mathematical results underlying this new theory. Candès and Wakin [3] discuss

sensing mechanics in which a signal $f(t)$ is stored using inner product with linear functions, as shown in Equation 1.

$$y_k = \langle f(t), \phi_k(t) \rangle. \quad (1)$$

Specifically, given a n -dimensional k -sparse signal S , we aim to find a $m \times n$ measurement matrix Φ_Ω and solve the optimization problem presented in the Equation 2.

$$\begin{aligned} & \min \|S\|_{l_1}, \\ & \text{subject to } \Phi_\Omega S = Y \end{aligned} \quad (2)$$

The components y_1, \dots, y_m of the Y vector are called measurements of the signal S , and Ω is a random measurement subset of size $|\Omega| = m$. Compressive Sensing (CS) theory aims to choose Φ_Ω to take as little measurements as possible and yet, to produce a reliable reconstruction of S .

Most times, a signal X must be rewritten as ($\Psi X = S$) in a proper basis in order to have a sparse representation, where Ψ is a change of basis matrix. Thus, instead of S in Equation 2, we have:

$$\begin{aligned} \Psi X = S & \iff \Psi^* S = X \\ \Theta_\Omega S = Y, & \text{ where } \Theta_\Omega = \Phi_\Omega \Psi^* \end{aligned}$$

Many natural signals such as images, sounds and, specially, geometrical meshes are sparse or they have a sparse representation in a proper basis. We explore, in this work, an approach that uses this new acquisition paradigm (*Compressive Sensing*) applied to geometric meshes. Thus, we can achieve a sparse representation, and use it a descriptor in a 3D CBIR context.

A. Spectral transformation

As described in Biscaro and Lima [4], our algorithm decomposes the mesh into two data sets: vertices and faces. We focused our study on the mesh geometry, i.e., the set of vertices. Thus, the set of faces was kept the same previous set. We decompose the set of vertices into three vectors called X , Y and Z , each one representing the data set of vertices in an axis of \mathbb{R}^3 . However, the data from these vectors are not in a sparse representation. So, we need to perform a spectral decomposition using a Laplacian matrix defined as follows.

First, consider E the set of edges of a mesh M and let d_i be the number of immediate neighbors of a particular vertex v_i (the valence or degree of v_i). Let A be the adjacency or connectivity matrix of M , as shown in Equation 3.

$$A_{ij} = \begin{cases} 1, & \text{if } (v_i, v_j) \in E \\ 0, & \text{otherwise} \end{cases} \quad (3)$$

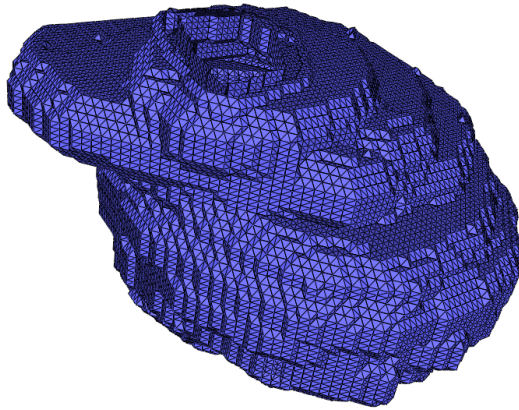
and let D be a diagonal matrix such that $D_{ii} = d_i$. Then, the Laplacian Matrix in relative coordinates is defined as:

$$L = I - D^{-1}A. \quad (4)$$

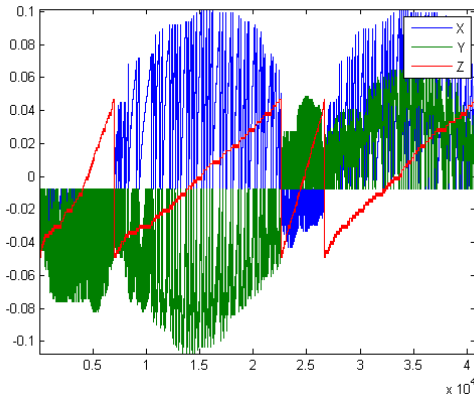
Next, we calculate the first k eigenvectors through a SVD decomposition, $L = U\Sigma V^*$ where U is an unitary matrix

$n \times k$; Σ is a $k \times k$ diagonal matrix and the $k \times n$ unitary matrix V^* denotes the conjugate transpose of $n \times k$ matrix V . Each vector X, Y and Z is multiplied by U to obtain a sparse representation.

An example of this approach is shown in Figures 2 and 3. Figure 2 shows an original object, where Figure 2b illustrates the dense nature of the vertices' coordinates. The x -axis represents the number of vertices while the y -axis represents the magnitude of the values. The blue, green and red colors are used to distinguish the axes X, Y and Z , respectively. Figure 3 shows the result of the spectral transformation, with $k = 300$. Figure 3a shows the reconstructed object from the 300 most significant coefficients. The coordinates become more sparse after applying the change of basis, as shown in Figure 3b.



(a)



(b)

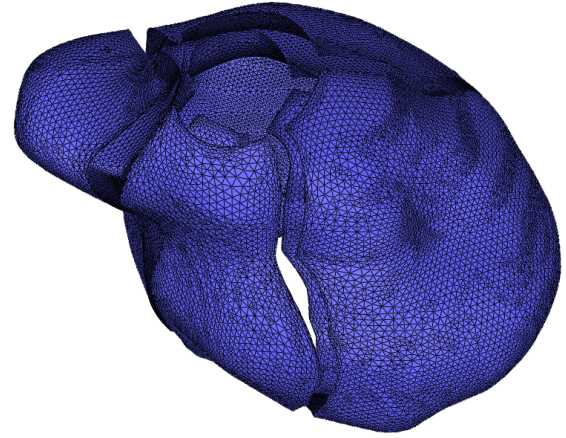
Fig. 2. Plot of the spectral and the Cartesian coordinates of a single mesh: (a) Original object: 40,789 vertices and 79,524 triangles. (b) Cartesian coordinates.

In this example we get a representation that requires only 0.73% of the initial amount of the object vertices.

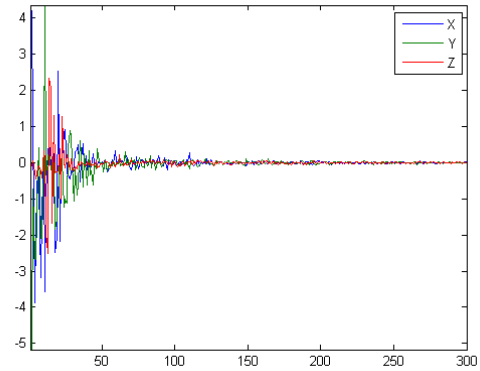
B. CBIR

In general, CBIR systems allow to retrieve in a database, the objects that are similar to an object provided as an input.

Almost every CBIR system can be performed in four stages: **Pre Processing; Feature Extraction; Similarity Comparison**



(a)



(b)

Fig. 3. Object after Compressive Sensing: (a) 3D reconstructed object. (b) Spectral coordinates.

and Relevance Feedback.

During the **Pre Processing** step, the image or the geometric object, in our case, investigated in order to prepare it to feature extraction. Techniques to remove noise and to enhance regions of interest are commonly used in this step.

In the **Feature Extraction** stage, the descriptors are developed. They are algorithms responsible for the low-level object description. Features such as color, shape, and texture are investigated and processed. Then, they are represented in a more comparative way, usually numbers. Thus, the set of features composes a “features vector”. Researchers have been studied faster and more robust extraction methods aiming to increase the accuracy of the CBIR systems [5]. The information resultant of this process is stored and indexed in a database system.

The step of **Similarity Comparison** aims to compute the difference between two objects based on their features. One of these objects is given as search parameter while the other is stored in the database system and had its features previously extracted. Distance functions are the simplest methods used in this step, but it is also possible to apply statistical techniques and other computational methods, such as artificial

intelligence. There are many ways to exhibit the results for users. In general, the most used is the ranking method, which presents thumbnail images sorted according to their similarity degree in relation the object provided as the query model. [6].

The **Relevance Feedback** is an optional step in the CBIR systems. It aims to decrease semantic gap existing between user and computer. Through an user evaluation about results presented is possible to refine the search and improve the tool precision [7].

C. Congestive Heart Failure

CHF is a common chronic cardiac disease which affects about 22 million people in the world and it is identified 2 million new cases [8] per year. This disease is related to the ventricles chambers dysfunctions, mainly on left ventricle.

The main characteristic of CHF is the inability of the heart achieve the demand of the different organ systems, causing an extra strain on the heart to supply this deficiency. In a long term, this overload could deform the ventricles structures [9]. These ventricle deformation are small and their identification requires the analysis of many two-dimensional slices of the images exam – usually MRI or CT. It is a difficult task, especially when the physician do not have much expertise on this subject.

III. RELATED WORKS

In recent years, particularly in medical field, CBIR systems focused in 3D domain have been little explored in the literature.

The work of Arya *et al.* [10] was one of the first to create a rudimentary 3D CBIR system for brain images. Their CBIR system had performance limitations due to the amount of data to be processed.

Yanxi and Dellaert [11] presented a weighted similarity metric based on Bayes decision theory. The authors applied their technique in recovering neuro-cardiological CT images for both healthy and injured brains. The methodology exploits the fact that the normal human brains present an approximate bilateral symmetry, which is often absent in pathological brains.

Cai, Feng and Fulton [12] presented a system for storage and retrieval of Positron Emission Tomography (PET). According to the authors, their system allows an efficient retrieval for content-based physiological and kinematic structures. However, their work was focused on specific structure retrieval (lungs).

Dong *et al.* [13] presented an approach that classifies the local structures in line-like, blob-like and sheet-like patterns. Such classification is performed based on second-order derivatives. The limitations of this approach are that the information extracted is not discriminative enough and that the technique needs to be adapted for each scenario that will be used.

In relation to cardiac problems, Glatard, Montagnat and Magnin [14] analyzed medical imaging properties and rated the Gabor filter aiming to perform clinically relevant queries on large image databases that do not require user supervision.

As a case study they used a set of cardiac images but their work just differentiates phases of the cardiac cycle.

In [15] Spherical Harmonics were used to map the left ventricle structure into a sphere. Then, by using the normalized and invariant sphere, the authors compare the left ventricles in two different states (dilated and relaxed). Since it was a preliminary study, they did not present a formal evaluation.

More recently, Ayary *et al.* [16] also used Spherical Harmonics to quantify deformations in different parts of the left ventricle in myocardial scintigraphy images, and this information was used to classify left ventricle structures in healthy or abnormal.

Related to the CHF specific disease, Bergamasco and Nunes [17] proposed a system for searching and retrieving clinical history based on 3D medical objects reconstructed from MRI Images to aid the diagnosis of congestive heart failure. Their work uses a local shape distance descriptor to retrieve 3D medical objects based on their deformations in specific locals. This provided a more precision retrieval, when compared to global approaches, since the problem analyzed (small deformations in the bottom of the left ventricle) requires a local approach.

In Bergamasco *et al.* [18] the same problem is addressed, however with a different approach to measure the similarity called Spectral Cluster (SC). To extract the features from the 3D objects, the authors use an adaptation of the Hough transform called 3D Hough Transform Descriptor (3DHTD). According to the authors, their approach reached 83% of overall accuracy. As an improvement of their previous work, Bergamasco *et al.* [19] used a bipartite graph technique in order to improve the retrieval precision. According to the authors, accuracy increased by 10% when compared to a method that use distance functions as similarity metric.

A. Sparse Representation of 3D Models

Research in 3D models sparse representation started to take off in the mid- to late-90s, and has been focused in compression algorithms. The 3D mesh information can be divided into geometric information, parameter information, and topology or connectivity information. The geometric information concerns the vertices coordinates and the normal vectors at the vertices; the parameter information refers to any information that can be stored in the mesh, for instance, color, heat information, forces, etc; the connectivity information is related to the neighborhood information among the vertices, the genus of the surfaces and so on.

Khodakovsky *et al.* [20] offer a progressive compression scheme that can handle arbitrary surface topology and highly detailed geometry. They use semi-regular wavelet transforms, zerotree coding and subdivision-based reconstruction scheme to improve their approach. Karni and Gotsman [21] project the x , y and z coordinate vectors onto basis functions to obtain a geometric spectrum for each coordinate. Those basis functions are, in fact, the Fourier basis functions. Therefore, encoding and decoding are performed by means of the Fast Fourier Transform (FFT). The connectivity is mapped on a

6-regular connectivity without using geometry information in the process. This approach is non-optimal, but provides an acceptable trade off between performance and computational cost.

The work of Du and Geng [22] provides a compressive sensing-based method for mesh compression by using a Laplace operator. According to the authors, the results are suitable for large-scale data compression; however, no experiments about BPV rates or PSNR [23] of the results are presented.

Krivokuca, Abdulla and Wünsche [24] have proposed a method for creating frames to be used as overcomplete dictionary for progressive compression of 3D mesh geometry. The authors obtained a sparse representation by decomposition of the mesh geometry onto orthogonal basis. Damkjer and Foroosh [25] presented an approach to work with larges cloud of points and also to preserve the objects features.

IV. METHODOLOGY

A. Materials

We used 27 cardiac objects to evaluate our approach. They were obtained by segmentation and reconstruction of sets of MRI images of the heart.

Each set of slices was segmented and reconstructed using the softwares Seg3D[26] and ImageVis[27], respectively. Figure 4 presents a step-by-step of the segmentation task and Figure 5 presents a surface reconstructed of the left ventricle.

In our objects set, 55% of the objects presented CHF and 45% were normal cases. 76.6% of the patients were over 40 years. These 3D objects were provided and classified as CHF and non-CHF case by experts of the Heart Institute (InCor), which is the largest medical center in Brazil that investigates cardiac diseases.

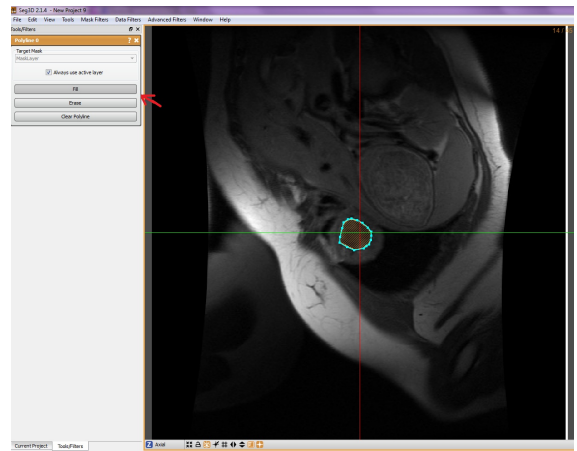
B. Implementation

The 3D objects loader, descriptors and similarity functions were implemented in Java language, using the Java3D library [28]. The Spectral Descriptor described in section II was implemented in Matlab environment [29]. Algorithm 1 illustrates the main steps of the process.

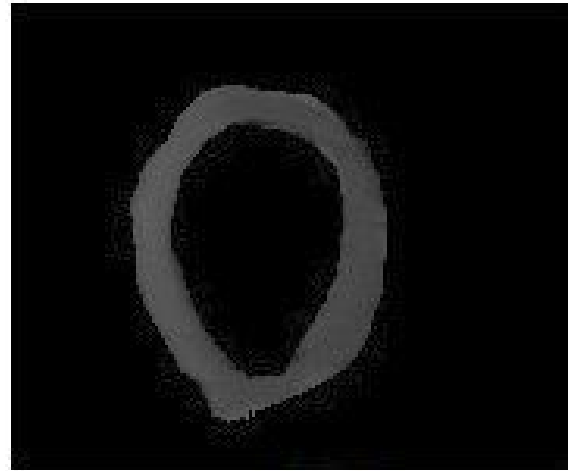
<p>Data: An ASCII file representing a Mesh M</p> <ol style="list-style-type: none"> 1 Create a matrix O_v with the mesh's vertices ; 2 Create a matrix O_f with the mesh's faces (connectivity) ; 3 Create a Laplacian Matrix L as described in section II ; 4 Compute the SVD decomposition of L; $L = U\Sigma V^*$; 5 Compute $SC = U * O_v$; 6 Write the vector SC in an output file;

Algorithm 1: Spectral Descriptor

The ASCII file that represent our meshes is usually in OFF format [30] and contains geometric information (vertices' coordinates) as well as connectivity information (mesh's faces). The output vector (line 6 of algorithm 1) is used as a feature vector in our Spectral Descriptor. The k value described



(a)



(b)

Fig. 4. Segmentation task: (a) manual segmentation (in blue color) of the left ventricle in a MRI slice; (b) segmented structure.

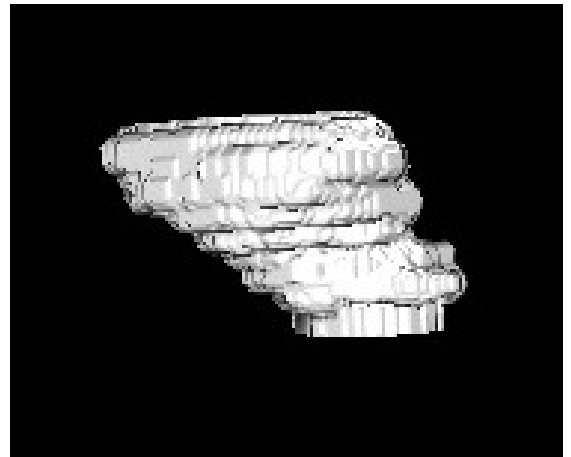


Fig. 5. 3D object of the left ventricle reconstructed.

in section II is responsible for selecting the first k largest eigenvalues of the Laplacian Matrix. The justification for this choice is due to the fact that the highest values contain most

of the information contained in the mesh.

C. Experiment and evaluation

We conducted an experiment composed by 6 tests performed on each of all the 27 objects reconstructed from the left ventricle, previously presented. We tested the retrieval for each object varying the coefficient k in 50, 100 and 200. For each value of k we tested the behavior of the retrieval by using Euclidean and Manhattan distance as similarity function.

The experiment was evaluated by the Precision *versus* Recall metric. Precision *versus* Recall is a metric widely used in CBIR context. Precision (Equation 5), for a specific class, can be described as a number of **true positives**, i.e., the number of items correctly labeled as belonging to the positive class, divided by the total number of elements labeled as belonging to the positive class (including the false positives). Recall (Equation 6) is the number of true positives divided by the total number of elements that actually belong to the positive class (the sum of true positives and false negatives) [31].

$$\text{Precision} = \frac{\text{relevant objects} \cap \text{retrieved objects}}{\text{retrieved objects}} \quad (5)$$

$$\text{Recall} = \frac{\text{relevant objects} \cap \text{retrieved objects}}{\text{relevant objects}} \quad (6)$$

V. RESULTS AND DISCUSSION

We obtained the average precision and we noted that retrieval of objects without CHF was better than retrieval of objects with CHF in any scenario: with different coefficients and both for Euclidean and Manhattan distance. Tables I and II detail the average precision for each similarity function. It is possible to note that the average precision of the retrieval using Manhattan Distance was 5% better than the retrieval using the Euclidean Distance.

TABLE I
AVERAGE PRECISION USING EUCLIDEAN DISTANCE

Coefficient	Average Precision - Euclidean Distance	
	CHF presence	Non-CHF
50	59,01%	81,69%
100	61,55%	82,91%
200	62,99%	83,28%

TABLE II
AVERAGE PRECISION USING MANHATTAN DISTANCE

Coefficient	Average Precision - Euclidean Distance	
	CHF presence	Non-CHF
50	67,23%	84,95%
100	68,40%	84,95%
200	70,57%	82,07%

Figures 6, 7 and 8 present the Precision vs. Recall curves from the results using Euclidean Distance. Figures 9, 10 and 11 show the Precision vs. Recall curves using Manhattan Distance.

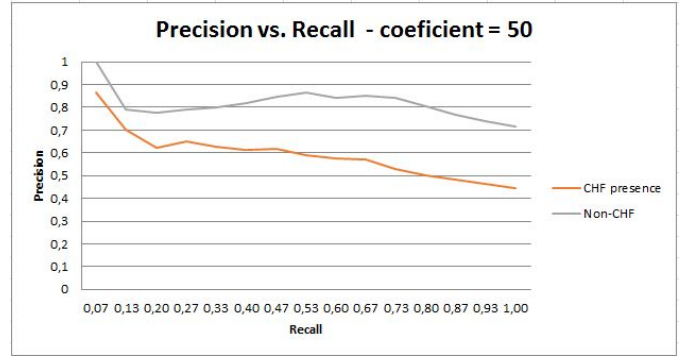


Fig. 6. Precision vs. Recall using Euclidean Distance and $k = 50$.

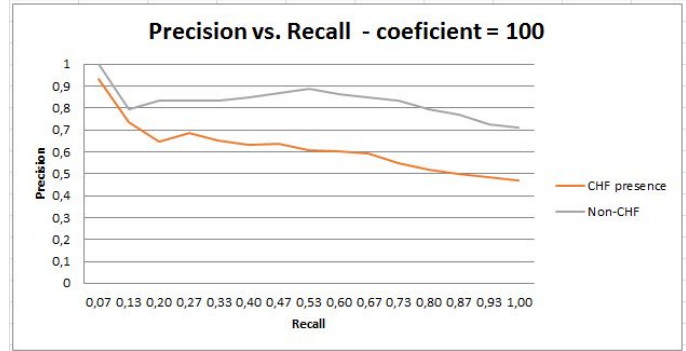


Fig. 7. Precision vs. Recall using Euclidean Distance and $k = 100$.

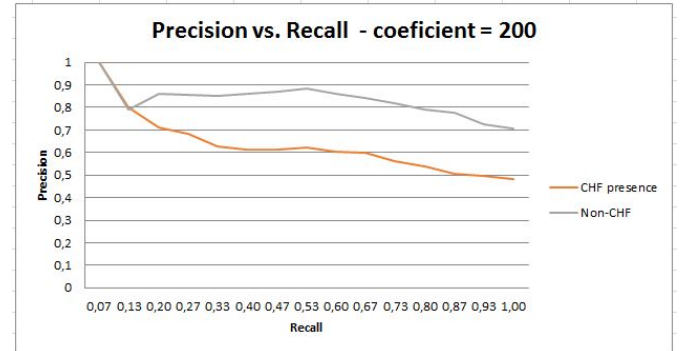


Fig. 8. Precision vs. Recall using Euclidean Distance and $k = 200$.

As aforementioned, the retrieval precision was better for non-CHF cases. It is possible to note that the descriptor presented high levels of precision (about 80%), even for high values of recall. This is a positive point of the proposed descriptor, since the most of descriptors decrease the performance to high values of recall, i.e., as the number of 3D objects retrieved increases, the precision tends to decrease, since the differences become smaller.

In the tests using Manhattan distance as similarity function and 200 coefficients we noted the best retrieval precision (70% for objects with CHF and 82% for objects without the anomaly). We also noted that the precision with Euclidean distance decreased on the second or third 3D object retrieval

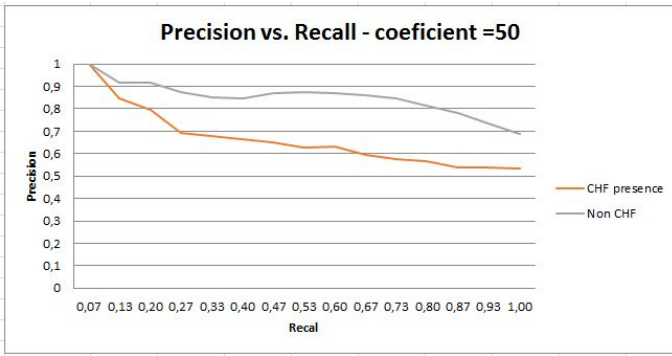


Fig. 9. Precision vs. Recall using Manhattan Distance and $k = 50$.

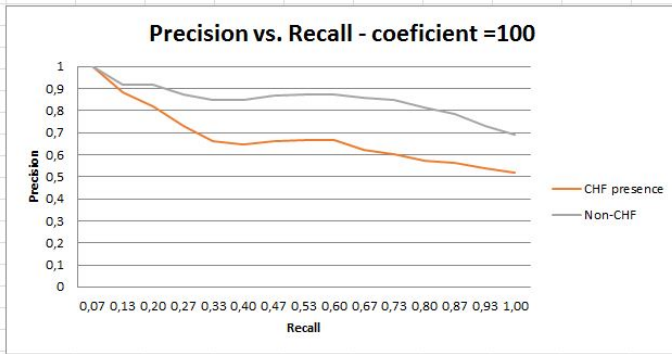


Fig. 10. Precision vs. Recall using Manhattan Distance and $k = 100$.

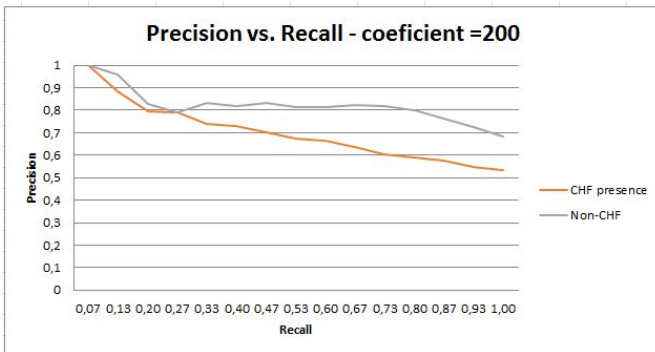


Fig. 11. Precision vs. Recall using Manhattan Distance and coefficient $k = 200$.

– this means that the CBIR system retrieved “wrong” case already in the beginning of the retrieval. This fact configures a bad performance, since usually it is easier for a descriptor to retrieve the most similar objects, which are related to small values of distances. By using Manhattan distance we noted retrieval mistakes just on the 4th or 5th 3D object retrieved.

The best performance obtained using Manhattan distance could be explained by the sparse nature of the descriptor vectors. The Manhattan distance is more precise as more sparse were the elements to compare since numerical accuracy problems with the calculation of the square root are avoided.

As mentioned before, our intention is investigate the Compressive Sensing theory as a possible approach to represent

3D objects in a suitable way for application in CBIR contexts. A regularly discussed problem in CBIR systems is the high dimensionality of the features vector. As shown in our experiment, the Spectral Descriptor, derived from the CS theory can be a suitable way to minimize this question, since the amount of coefficients can be adjusted according the characteristics of object. Although we intend conduct more experiments considering other objects, we realized that the retrieval precision does not increase proportionally to the increase in the number of coefficients. Thus, we can state that few numbers of coefficients can result in good precision rates, contributing to decrease the dimensionality of the features vector in CBIR problems. This happens just because we consider a sparse representation of the 3D object instead of consider all its vertices and faces.

Bergamasco and Nunes [32] proposed a novel approach based on 3D object shape information obtained by 3D Hough Transform. This descriptor also used Euclidean distance as similarity function and had the most precise results on their experiments, reaching 85% of precision in lower values of recall. Comparing our approach with results obtained in [32], we noted that our current approach overcomes the precision results. In their experiments, authors noted an average precision of 44% for CHF cases and 58% for non-CHF exams, while in this work we found 59% for CHF and 81% for non-CHF cases in the worst case.

VI. CONCLUSION AND FUTURE WORKS

This paper presented the use of the Compressive Sensing theory to develop a new descriptor aiming at improving retrieval in 3D CBIR systems. The descriptor was applied to retrieve 3D cardiac models to contribute to aid the CHF diagnosis. The coordinates of the compressed models were used to form the features vectors, representations of models which are compared using a similarity function to determine the similarity between two models. Our proposal makes a base change such that the coordinates of the vertices of a 3D model, which previously had a dense representation, can be rewritten on a basis of which have a sparse representation.

Our descriptor relay on a kind of “uncertainty principle” between a canonical basis and a measurement basis which states that a mesh, when interpreted as a signal, cannot have a dense representation in both basis at the same time.

Although still in early stages of testing, our descriptor proved useful in CBIR applications, particularly in our test environment with left ventricular heart models. The strength of the descriptor developed here was the identification of non-CHF models. The performance for cases with CHF can be further improved, for example by using a larger number of SVD decomposition on coefficients as well as the use of more accurate three-dimensional models.

Additionally, our descriptor must be tested in a more varied set of templates in order to confirm its potential as a tool to improve CBIR systems performance. Additionally, as future work we intend to test our approach with models that comprises another anomalies as well as other types of

3D models. We also planning conduct a complete comparison of this spectral descriptor with other descriptors in order to evaluate not only its precision, but also the response time and the memory and storage requirements.

In this work, we compare our results considering the results of a descriptor previously developed which retrieved similar objects in a CBIR system. Another possibility for improving this study is to compare the technique used for obtaining the sparse representation of mesh with other techniques found in the literature cited in the section III, as well as conducting additional tests from variation of the parameters of the technique presented here.

ACKNOWLEDGMENT

Authors are grateful to Brazilian Ministry of Education, to the National Institute of Science and Technology Medicine Assisted by Scientific Computing, National Council for Scientific and Technological Development (CNPq), and São Paulo Research Foundation (Fapesp), for the financial support, as well as to the Heart Institute (InCor) and Professor Carlos Eduardo Rochitte, for providing the images.

REFERENCES

- [1] A. Schulz, L. Velho, and E. A. B. Da Silva, "On the empirical rate-distortion performance of compressive sensing," in *Proceedings of the 16th IEEE International Conference on Image Processing*, ser. ICIP'09. Piscataway, NJ, USA: IEEE Press, 2009, pp. 3013–3016.
- [2] E. J. Candès, J. Romberg, and T. Tao, "Robust uncertainty principles: Exact signal reconstruction from highly incomplete frequency information," *IEEE Trans. Inform. Theory*, vol. 52, no. 2, pp. 489–509, 2006.
- [3] E. Candès and J. Romberg, "Sparsity and incoherence in compressive sampling," *Inverse Problems*, vol. 23, pp. 969–985, 2007.
- [4] H. H. Biscaro and J. P. Lima, "Compressive representation of three-dimensional models," *Journal on Interactive Systems*, vol. 6, no. 1, pp. 1–8, 2015.
- [5] S.-F. Chang, T. Sikora, and A. Purl, "Overview of the mpeg-7 standard," *Circuits and Systems for Video Technology, IEEE Transactions on*, vol. 11, no. 6, pp. 688–695, Jun 2001.
- [6] R. D. S. Torres and A. X. Falcão, "Content-based image retrieval: Theory and applications," *Revista de Informática Teórica e Aplicada*, vol. 13, pp. 161–185, 2006.
- [7] Z. Qin, J. Jia, and J. Qin, "Content based 3D model retrieval: A survey," in *Content-Based Multimedia Indexing, 2008. CBMI 2008. International Workshop on*, June 2008, pp. 249–256.
- [8] AHA – American Heart Association, "Heart failure," 2015, Available at: <http://www.heart.org>.
- [9] A. Banerjee, A. M. Mendelsohn, T. K. Knillans, R. A. Meyer, and D. C. Schwartz, "Effect of myocardial hypertrophy on systolic and diastolic function in children: insights from the force-frequency and relaxation-frequency relationships," *Journal of the American College of Cardiology*, vol. 32, no. 4, pp. 1088 – 1095, 1998.
- [10] M. Arya, W. Cody, C. Faloutsos, J. Richardson, and A. Toga, "Qbism: extending a dbms to support 3d medical images," in *Data Engineering, 1994. Proceedings. 10th International Conference*, Feb 1994, pp. 314–325.
- [11] Y. Liu and F. Dellaert, "A classification based similarity metric for 3d image retrieval," in *Computer Vision and Pattern Recognition, 1998. Proceedings. 1998 IEEE Computer Society Conference on*, Jun 1998, pp. 800–805.
- [12] W. Cai, D. Feng, and R. Fulton, "Content-based retrieval of dynamic PET functional images," *Information Technology in Biomedicine, IEEE Transactions on*, vol. 4, no. 2, pp. 152–158, June 2000.
- [13] S. Dong, K. Dong, and L. Yin, "The application of local structure classification in content-based 3d medical image retrieval," in *Image and Graphics (ICIG), 2013 Seventh International Conference on*, July 2013, pp. 639–642.
- [14] T. Glatard, J. Montagnat, and I. E. Magnin, "Texture based medical image indexing and retrieval: Application to cardiac imaging," in *Proceedings of the 6th ACM SIGMM International Workshop on Multimedia Information Retrieval*, ser. MIR '04. New York, NY, USA: ACM, 2004, pp. 135–142.
- [15] W. B. H. Khelifa, A. Ben Abdallah, and F. Ghorbel, "Three dimensional modeling of the left ventricle of the heart using spherical harmonic analysis," in *Biomedical Imaging: From Nano to Macro, 2008. ISBI 2008. 5th IEEE International Symposium on*, 2008, pp. 1275–1278.
- [16] R. Ayari, A. B. Abdallah, R. Sfar, F. Ghorbel, and M. H. Bedoui, "Analysis of regional deformation of the heart's left ventricle using invariant SPHARM descriptors," *IRBM*, vol. 35, no. 5, pp. 226 – 232, 2014.
- [17] L. C. C. Bergamasco and F. L. S. Nunes, "A new local feature extraction approach for content-based 3d medical model retrieval using shape descriptor," in *Proceedings of the 29th Annual ACM Symposium on Applied Computing*, ser. SAC '14. New York, NY, USA: ACM, 2014, pp. 902–907.
- [18] L. Bergamasco, R. Oliveira, H. Wechsler, C. Dajuda, M. Delamaro, and F. Nunes, "Content-based image retrieval of 3d cardiac models to aid the diagnosis of congestive heart failure by using spectral clustering," in *Computer-Based Medical Systems (CBMS), 2015 IEEE 28th International Symposium on*, June 2015, pp. 183–186.
- [19] L. Bergamasco, H. Oliveira, H. Biscaro, H. Wechsler, and F. Nunes, "Using bipartite graphs for 3d cardiac model retrieval," in *Computer-Based Medical Systems (CBMS), 2015 IEEE 28th International Symposium on*, June 2015, pp. 232–237.
- [20] A. Khodakovskiy, P. Schröder, and W. Sweldens, "Progressive geometry compression," *SIGGRAPH '00 Proceedings of the 27th annual conference on Computer graphics and interactive techniques*, pp. 271–278, 2000.
- [21] Z. Karni and C. Gotsman, "3d mesh compression using fixed spectral bases," in *No description on Graphics interface 2001*, ser. GRIN'01. Toronto, Ont., Canada, Canada: Canadian Information Processing Society, 2001, pp. 1–8.
- [22] Z.-M. Du and G.-H. Geng, "3-D geometric signal compression method based on compressed sensing," in *Image Analysis and Signal Processing (IASP), 2011 International Conference on*, 2011, pp. 62–66.
- [23] G. Peyré, "Fourier on meshes," 2008, acesso em Novembro de 2013.
- [24] M. Krivokuca, W. H. Abdulla, and B. C. Wünsche, "Sparse approximations of 3d mesh geometry using frames as overcomplete dictionaries," in *Computer Vision Workshops (ICCVW), 2013 IEEE International Conference on*, Dec 2013, pp. 660–667.
- [25] K. L. Damkjer and H. Foroosh, "Mesh-free sparse representation of multidimensional lidar data," in *Image Processing (ICIP), 2014 IEEE International Conference on*, Oct 2014.
- [26] CBIC. (2012) Seg3D: Volumetric Image Segmentation and Visualization. Scientific Computing and Imaging Institute (SCI). Disponível em: <http://www.seg3d.org>.
- [27] ——. (2012) ImageVis3D: A Real-time Volume Rendering Tool for Large Data. Scientific Computing and Imaging Institute (SCI). Disponível em: <http://www.imagevis3d.org>.
- [28] Java3D, "Java3D," [%urlhttp://www.oracle.com/technetwork/articles/javase/index-jsp-138252.html](http://www.oracle.com/technetwork/articles/javase/index-jsp-138252.html), 2015, acessado em: 03 out. 2015.
- [29] MATLAB, version 7.10.0 (R2010a). Natick, Massachusetts: The MathWorks Inc., 2010.
- [30] N. Amenta, S. Levy, T. Munzner, and M. Phillips, "Geomview: A system for geometric visualization," *Communication to the Proceedings of the 11th Annual ACM Symposium on Computational Geometry*, pp. C12–13, 1995.
- [31] A. W. M. Smeulders, M. Worring, S. Santini, A. Gupta, and R. Jain, "Content-based image retrieval at the end of the early years," *Pattern Analysis and Machine Intelligence, IEEE Transactions on*, vol. 22, no. 12, pp. 1349–1380, 2000.
- [32] L. C. Bergamasco and F. L. Nunes, "Three-dimensional content-based cardiac image retrieval using global and local descriptors," in *AMIA Annual Symposium Proceedings*, vol. 2015. American Medical Informatics Association, 2015, p. 1811.